*Annals of Biomedical Engineering*, Vol. 21, pp. 33–43, 1993
Printed in the USA. 

0090-6964/93 $6.00 + .00


# Computer-Aided Vascular Experimentation: A New Electromechanical Test System

J.D. HUMPHREY, T. KANG, P. SAKARDA, and M. ANJANAPPA

Department of Mechanical Engineering, The University of Maryland, Baltimore MD

**Abstract**—We present a new computer-controlled, electromechanical system for performing simultaneous extension, inflation, and torsion experiments on cylindrical segments of natural and artificial blood vessels. Specimens are tested while immersed in a temperature-controlled, oxygenated, physiologic solution. Deformations are measured within a central region of the specimen using noncontacting video methods. The associated axial loads, luminal pressures, and torques are measured with standard transducers. Data are collected and stored online, and are used in the feedback control of experimental protocols, which are prescribed using custom interactive software. Finally, we present illustrative data obtained from canine aortas and common carotid arteries.

**Keywords**—Constitutive relations, Biomechanics, Arteries.

## INTRODUCTION

Although there is a huge literature on the mechanics of blood vessels (1,2,14,29), many important questions remain in vascular pathophysiology and surgery. For example, intramural stresses are thought to play important roles in the failure of vascular grafts (25,33), the development and rupture of aneurysms (26,30), the damage that results from balloon angioplasty (3,4,22) and from balloon embolectomy (9,15), and in atherogenesis (12,36). Nonetheless, the mechanical mechanisms operative in these examples are not well understood, and optimal clinical methods remain unknown. One reason for this is that the associated stress analyses have not been rigorously performed, primarily due to the lack of complete three-dimensional constitutive relations for blood vessels.

Identification of reliable constitutive relations depends largely upon good data, and hence on good experimental equipment and techniques. *In vivo* data (e.g., pressure-diameter) provide useful information on vascular behavior, but are not sufficient for the rigorous determination of a constitutive relation. Interpretation of *in vivo* data is complicated by the presence of unquantified boundary conditions (e.g., perivascular tethering), the difficulty of separating compensatory reflexes from biomechanical responses, and the difficulty of measuring and controlling axial deformations and forces (5,11,21,27,39). Fortunately, neither anesthesia (6) nor excision (21) appears to affect the mechanical properties of blood vessels; thus *in vitro* tests can be used to study *in vivo* behavior.

Excised vessels can be tested as uniaxial strips (23,46), small rings (4,7,32), flat sheets (24), or cylindrical segments (5,8,13,20,37,39,40,42–44). Tests on cylindrical specimens preserve the *in vivo* ultrastructure, and can better mimic physiological loading conditions. Hence they are the preferred tests (5,7,39,40). Humphrey *et al.* (18) recently suggested that in addition to *in vitro* tests that mimic physiologic loads, more sophisticated extension, inflation, and torsion experiments may be needed to better quantify the complex biomechanical behavior exhibited by blood vessels. Due to the complexity of the proposed experiments, however, no existing device was capable of performing the tests. Thus, the specific aim of this work was to design and assemble a new computer-controlled, electromechanical system capable of performing simultaneous extension, inflation, and torsion experiments on cylindrical segments of excised blood vessels. We describe our system here, and present illustrative data from experiments on canine aortas and common carotid arteries.

## EXPERIMENTAL SYSTEM

The complete system consists of three sub-systems: an electro-mechanical device, a video-based deformation

*Acknowledgment*—This article is dedicated to the memory of Dr. Bernard J. McCaffrey, late Professor at UMBC, true experimentalist and friend.

This project was funded by a grant from The Whitaker Foundation for which we are most grateful. We also wish to acknowledge Mr. John Toeneboehn, who accomplished much of the original mechanical design as part of a senior project; Mr. William W. Calary, who suggested many clever design changes and who did the machining; and Mr. John Downs, who helped with the software development and hardware installation. Finally, our thanks to Dr. Frank Yin for many insightful comments.

Address correspondence to Jay D. Humphrey, Dept of Mechanical Engineering, The University of Maryland, 5401 Wilkens Avenue, Baltimore, MD 21228-5398.

*(Received 1/23/91; Revised 10/15/91)*

measurement system, and a control and data acquisition system.[1]

*Device*

A top view line drawing (Fig. 1) of the electro-mechanical device reveals that it consists of a horizontally oriented, low friction, twin-shaft web assembly (H). The shaft assembly is 112 cm long, and is supported on both ends (R) and in the middle (not shown). Two 10 × 15 cm aluminum carriages (Q) ride on the shaft assembly on self-aligning linear ball bearings. These carriages are driven in opposing directions by a digital stepper motor (G) via left- and right-hand threaded ball screws (B); this arrangement keeps the stretching center fixed. The ball screws are attached to the carriages with ball nuts (C) and aluminum brackets, they are supported on each end by oil-impregnated bronze thrust bearings (A), and they are connected to each other, and to the motor, with wafer couplings (E). Adjustable limit switches restrict the allowable range of motion of the carriages.

Mounted atop the carriages is a linear variable differential transformer, or LVDT (D), which measures the distance between the carriages. Mounted on the front faces of the carriages are a second stepper motor (P) and three load cells, i.e., a pressure (I), a tension-compression axial load (J), and a torque (O) transducer. This second stepper motor is used to twist the specimen. The centerline of the pressure transducer coincides with that of the specimen, thereby alleviating the need to correct for differences in fluid heads. Moreover, since the pressure transducer rides on one of the carriages, the tubing between it and the specimen moves as a rigid body (i.e., it is never

[1]Detailed equipment and parts lists, including manufacturers' addresses, are available from the first author.

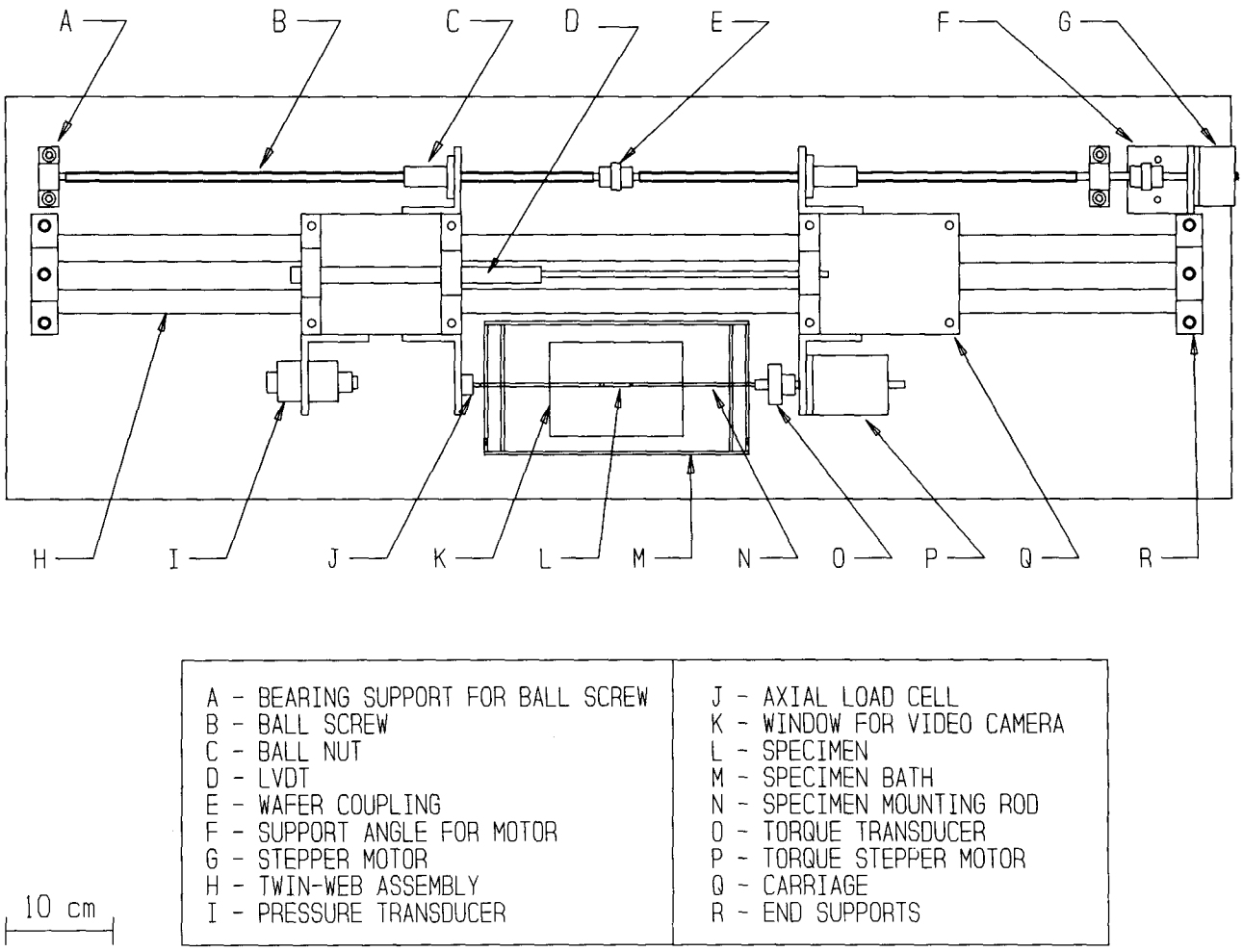


**FIGURE 1. Top view line drawing of our electromechanical device. Cables, tubing and the four limit switches are not shown for clarity.**

stretched, bent or twisted). Transducers with different ranges can be interchanged and aligned easily via individual aluminum mounting brackets.

Cylindrical specimens (L) are coupled to the device using 1.6 cm diameter Plexiglas mounting rods (N). Connected directly to the axial load and torque transducers, these mounting rods have a side port and an inner lumen through which fluid or catheters can be introduced into the specimen. Moreover, the mounting rods accept interchangeable "end adapters" of various diameters to accommodate different size vessels. The adapters insert into the ends of the mounting rods and are held in place by a size 5 O-ring and a set screw. Note, too, that the mounting rods go through holes (with 1 mm clearance) in the sides of the Plexiglas testing bath (M). The bath has an inner chamber which can be filled with a temperature-controlled physiologic solution using a heater-circulator pump (not shown), and an outer chamber which collects fluid that leaks out around the mounting rods. The outer chamber is emptied continuously using a standard roller pump, and the back of the bath consists of a 10 cm high splash-guard which protects the shaft assembly and ball screws from the salt solution.

A front view of the electromechanical system (Fig. 2) reveals that the device rests on a 38 × 117 × 1.3 cm aluminum base plate (T). This plate is positioned 15 cm above the top of a 91 × 122 cm optical table (P) using 16 supporting rods (S). A 9 × 15 cm cut-out in the plate (K in Fig. 1) allows the central region of the specimen to be viewed from underneath using a CCD camera (O) and a

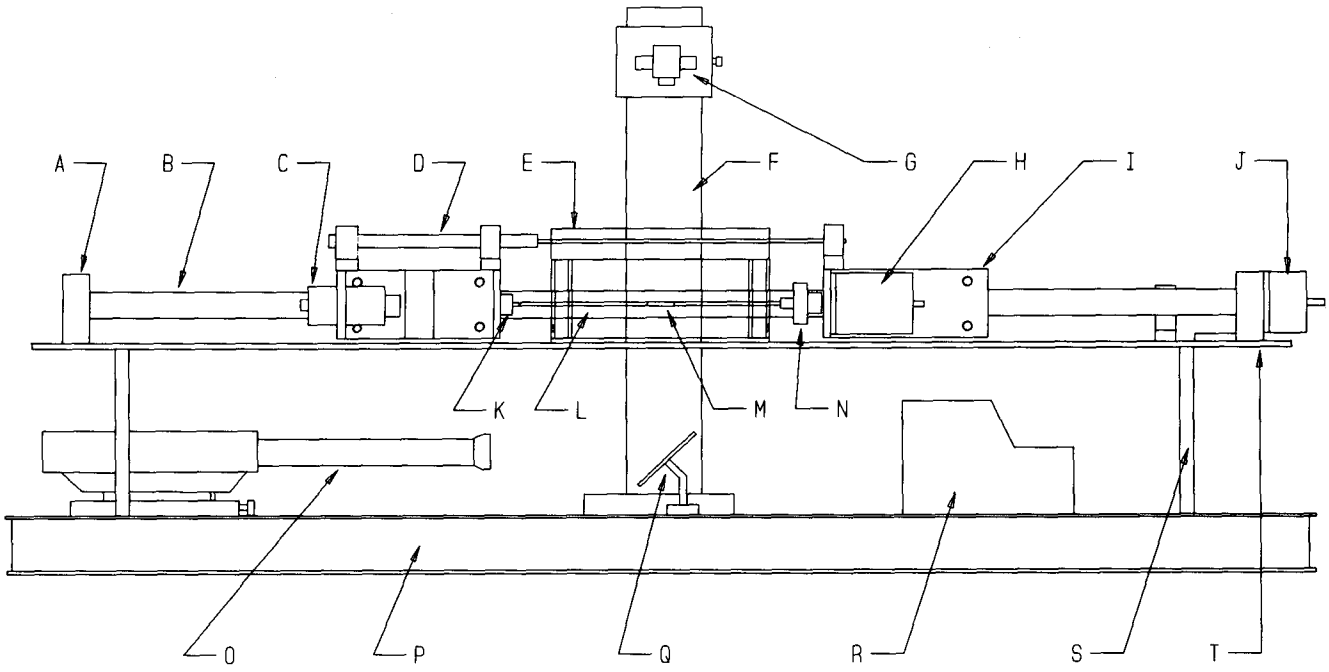


| | |
|---|---|
| A - END SUPPORTS | K - AXIAL LOAD CELL |
| B - TWIN-WEB ASSEMBLY | L - SPECIMEN MOUNTING ROD |
| C - PRESSURE TRANSDUCER | M - SPECIMEN |
| D - LVDT | N - TORQUE TRANSDUCER |
| E - SPECIMEN BATH | O - VIDEO CAMERA |
| F - MOUNTING COLUMN FOR VIDEO | P - OPTICAL TABLE |
| G - X-Y STAGE | Q - MIRROR |
| H - TORQUE MOTOR | R - DIGITAL PUMP |
| I - CARRIAGE | S - SUPPORT ROD |
| J - STEPPER MOTOR | T - BASE PLATE |

10 cm

**FIGURE 2. Front view line drawing of the device shown in Fig. 1. Not shown are the tubing, aspirator bottle, and fluid reservoir used in the vessel inflation, or the heater-circulator pump and roller pump used to maintain the bath fluid level. Similarly, not all of the supporting rods are shown.**

10 mm diameter optical mirror (Q) that is oriented at 45°. The camera is mounted on a 30 cm long optical rail, thereby allowing adjustment of the linear position of the camera. The optical center and stretching axis center are currently within 0.03 mm. A second camera can be mounted above the specimen, normal to the experimental plane, on a xyz stage (G) if desired. Whereas the LVDT (D) provides information on overall length changes of the specimen, the CCD cameras provide noncontacting information on the deformation of the specimen in a central region (i.e., gage length). This is important, of course, since it minimizes "end effects." A block diagram of the entire experimental system (Fig. 3) illustrates the relation of the mechanical device, shown in the center, to the video system and the control computer.

*Deformation Measurement*

The output signal from either the above, or below, mounted camera is fed to both a video dimension analyzer (VDA) (45) and associated B&W monitor and a video frame grabber board in a dedicated 386/20 PC (with a second B&W monitor). The VDA is used to monitor the "inflation" of the specimen in the central region, its output being a voltage that is directly proportional to the external diameter of the specimen. VDAs are commonly used in vascular experimentation (11–13,16,35,44).

A video system consisting of a dedicated 386/20 PC, a frame-grabber board, and custom software (10) is used to track small markers affixed to the surface of the vessel within a central gage length. The video image of the central region is digitized into a 512 × 512 "x-y" pixel array, each pixel having values from 0 (black) to 255 (white). The marker positions are first identified on the B&W monitor using a mouse cursor, and then are tracked using a correlation-based algorithm, which identifies subsequent locations within search regions that are centered about the last recorded marker position. The x,y coordinates of up to 4 markers can be determined at the 30 Hz video frame rate. Typical resolution is 58 pixels/mm, although

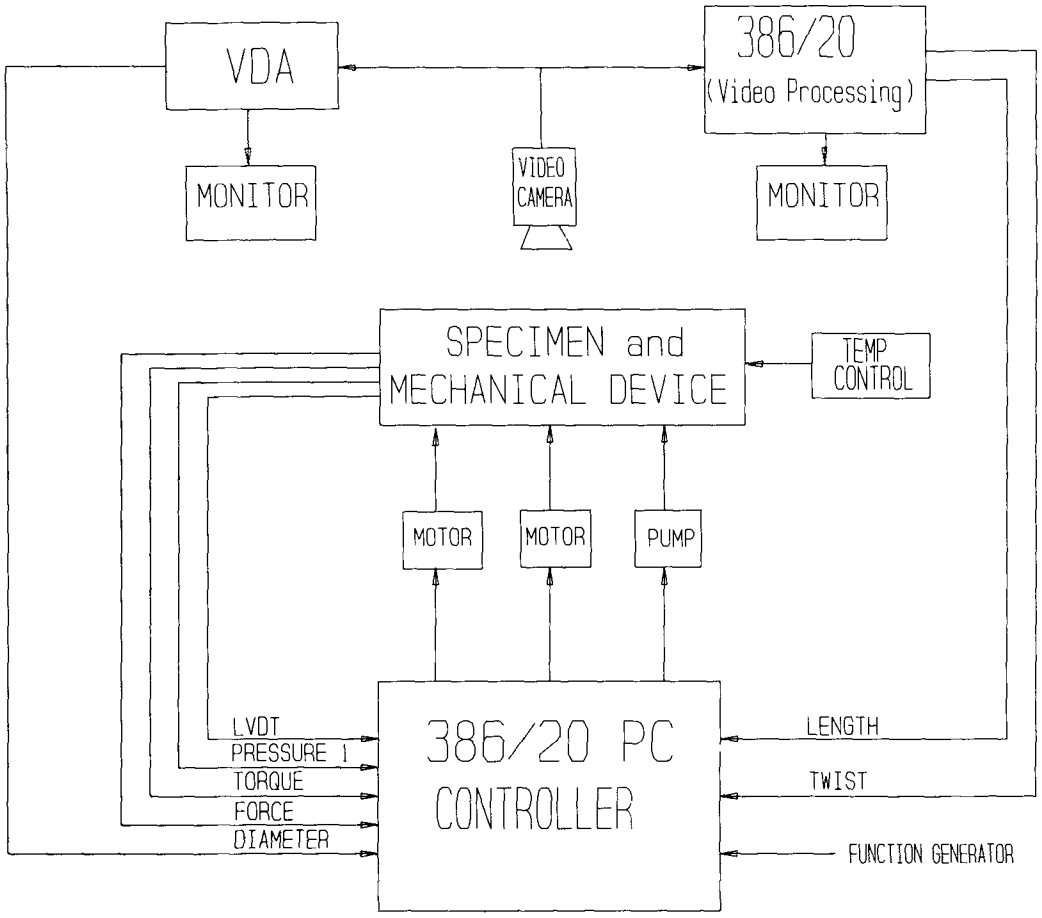


**FIGURE 3. Schema of the overall system. The motors are controlled via a board in the controller PC and two drivers (not shown). The fluid pump communication is through a serial port. The six analog signals are digitized on-line with an A/D board and the gage length and twist are calculated in the controller PC based on the four pairs of "x-y" coordinates of the tracking markers which come from the video processing PC.**

this can be modified as needed with changes in the optics. We use various combinations of extension tubes and 2× converters with either a 100 or a 200 mm macro lens. Since the vessels are typically white, a mat black background, with normal room lighting augmented with soft fiber optic light sources, is usually adequate for tracking purposes.

### *Data Acquisition and Experimental Control*

A second 386/20 PC acquires and stores the experimental data, and controls the experimental protocols (Fig. 3). Analog signals from the load cells (axial load, torque, pressure), LVDT, VDA, and an external function generator are amplified and then read via DMA transfers in a background mode with a 12 bit programmable A/D convertor. The function generator provides a known time varying signal to which the frequency of the cyclic data can be compared. The accuracy of the load cells and the LVDT is 0.1 to 0.2% full scale, and typical resolutions are 0.5 g, 1.75 g-cm, 0.65 mmHg, 0.1 mm (LVDT), and 0.02 mm (VDA). The gage length extension and twist of the specimen are calculated from the x-y coordinates (integers) of the two-to-four tracking markers. The coordinates are transferred to the control computer from the video computer using two 16 bit parallel boards. The A/D conversion and the coordinate transfers are synchronized, and hence the loads and the associated deformations are available for on-line storage, processing, and feedback control of the protocols.

The inflation, extension, and twist of the specimen are induced by a Harvard Apparatus peristaltic pump (R in Fig. 2) and two Compumotor stepper motors (J and H in Fig. 2), respectively. The pump dispenses fluid proportional to the steps moved by its own microstepper motor, and is controlled by ASCII commands sent from the control PC to the pump's microprocessor at 9600 baud via a RS-232 serial port. Currently, the fluid is pumped to the specimen through an intermediate half-filled glass aspirator bottle; this decreases the pulsatile character of the specimen inflation. The Compumotor motion system consists of the two motors, a PC23 indexer (i.e., board), and two drivers. The motors are controlled by commands sent from the PC to the PC23. The stepper motor used for the axial extension utilizes built-in sensors and PID feedback control algorithms to correct for desired positions and velocities. Axial positioning error is 0.1% up to 13 cm of travel and backlash error is 0.42 mm. The stepper motor used to twist the specimen is open loop in design, but can be controlled closed-loop in software. The associated rotational position accuracy is 0.1°.

All experimental protocols are executed through software as defined by the user via an interactive, custom, menu driven C program which controls the three actuators and the data collection. Utility routines allow on-line calibration of the data channels, individual precise control of the motors and pump, and on-line display of the 14 data channels; this simplifies experimental setup and execution greatly. Finally, in addition to hardware limit switches, which restrict the motion of the carriages, various software limits can be set to stop a test if preselected load or deformation limits are exceeded. This protects both the specimen and the device.

## ILLUSTRATIVE DATA

The ability to simultaneously extend, inflate, and twist a cylindrical specimen provides an experimentalist with an almost unlimited choice of possible protocols that can be performed. Rather than demonstrating many of the possible tests, we present only representative data from three classes of tests which were performed on canine common carotid arteries and aortas. All vessels were harvested from animals that were used in separate Institutional Animal Care and Use Committee approved protocols. Data were collected at 30 Hz following preconditioning (14), but a reduced number of data points are plotted for clarity.

### *Specimen Preparation*

Loose connective tissue was removed from the adventitial surfaces by gentle dissection, and the vessels were trimmed to 3–4 cm in length. Two to four small black tracking markers (i.e., ~200 $\mu$m diameter dried vanilla bean specks) were glued onto the specimen within a central region and along the centerline. The unloaded gage length and diameter were recorded using the video system by placing the vessel in the specimen bath and in the same optical plane as during the tests. Specimens were then removed from the bath, cannulated with appropriately sized end adapters, and secured with OOO suture. The cannulated specimen was placed in the device by inserting the end adapters into the ends of the mounting rods. Recall that the adapters are held in place by set screws and an O-ring. Fixed in this way, the adapter pull-out force is much greater than the maximum allowed axial loads. Finally, the vessel was purged of air by pumping fluid through one mounting rod while allowing the fluid to flow out of a tube in the other mounting rod. A modified stopcock was used to close the exit tube.

### *Carotids*

Similar to (6), common carotid arteries were tested at 37°C in an oxygenated $Ca^{++}$-free Krebs solution containing 2 mM EGTA. Shown in Figs. 4a–4d and 5a are data from tests,[2] wherein the axial stretch ratio $\lambda$ was

[2]See Humphrey *et al.* (18) for a detailed quantitative description of the experiments. Note, however, that the axial stretch ratio, $\lambda$, is defined as the ratio of the current to the unloaded gage length. *In situ* values of $\lambda$ typically range from 1.4 to 1.6.

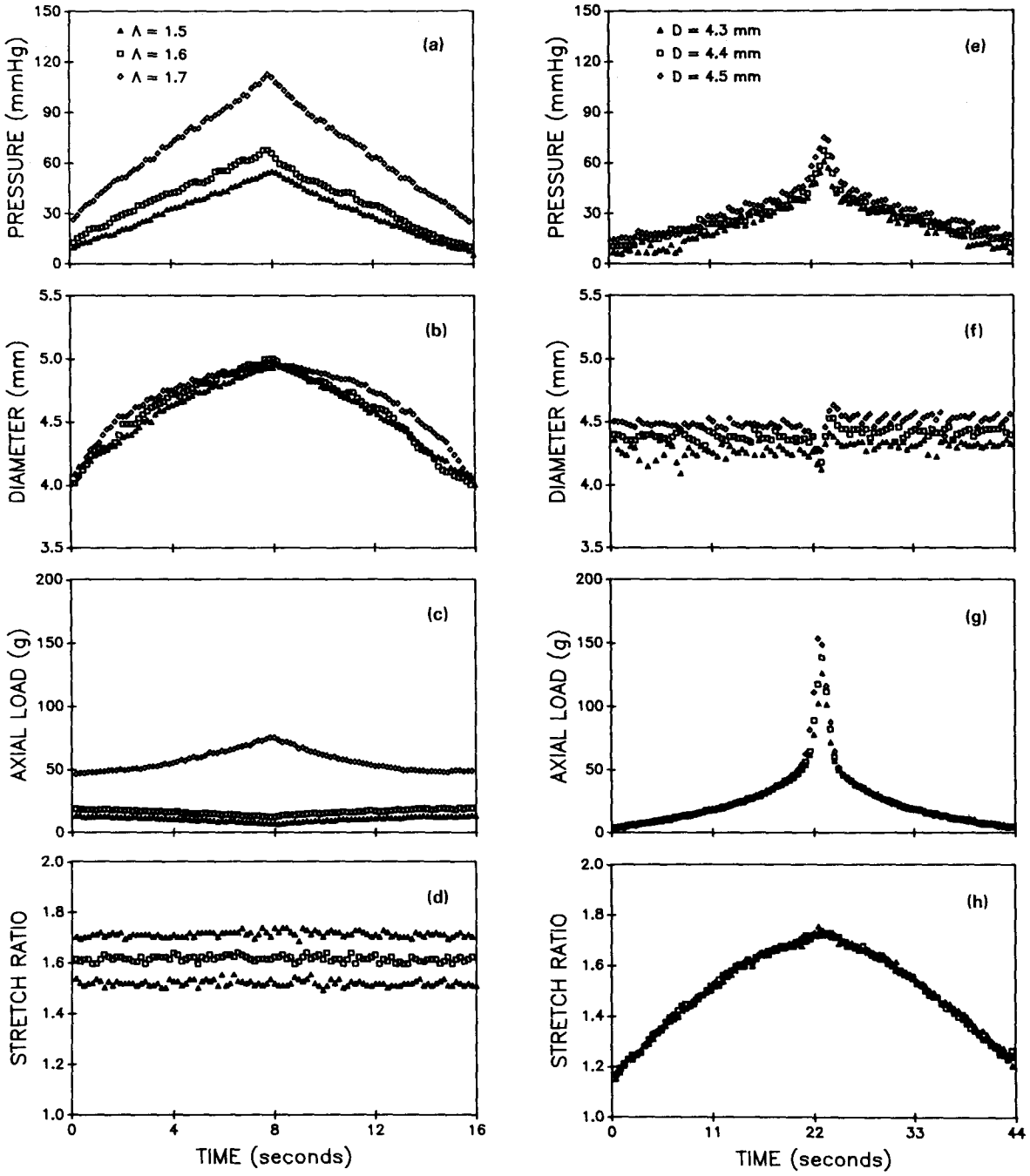


**FIGURE 4. Complete cycles of pressure, external diameter, axial load and axial stretch ratio data for a canine carotid artery subjected to six different tests. (a), (b), (c), and (d) show data from three different "constant axial extension" tests, whereas (e), (f), (g), and (h) show data from three "constant diameter" tests.**

separately maintained constant at three different prescribed values ($\Lambda = 1.5$, 1.6, and 1.7) while the vessel was cyclically inflated ($4.0 \leq D \leq 5.0$ mm) with the EGTA solution. Similarly, data from tests wherein the external diameter D (within the gage length) was separately maintained fixed at three different prescribed values ($D = 4.3$, 4.4 and 4.5 mm) while the vessel was cyclically extended ($1.15 \leq \Lambda \leq 1.7$), are in Figs. 4e–4h and 5b. The data were not filtered in any way.

Consider first the constant stretch ratio tests. For each, we show one complete cycle of the luminal pressure (Fig. 4a), the external diameter (Fig. 4b), the nearly constant axial stretch ratio (Fig. 4d), and the axial load (Fig. 4c) required to maintain the gage length constant,

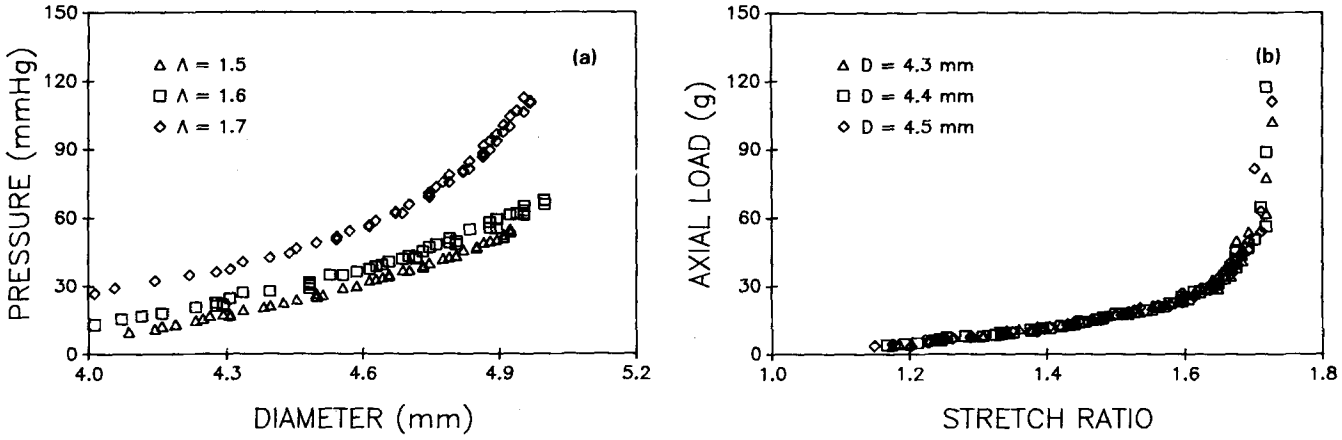


**FIGURE 5. Pressure-diameter plot (a) of the data in Figs. 4(a-d), and axial load-extension behavior (b) for the data in Figs. 4(e-h).**

all plotted vs. time. The pressure loading was prescribed to be linear in time similar to other studies (e.g., 5), but could have been prescribed differently. The axial load required to maintain the gage length constant either decreased or increased with increasing luminal pressure depending on whether Λ was less than or greater than the *in situ* value. The converse was true for decreasing luminal pressure. This is a commonly observed behavior (35,43). The data are replotted as pressure vs. diameter in Fig. 5a for the three values of constant axial stretch. The nonlinear pressure-diameter response, which shows a stiffening behavior with increased axial extension, is also consistent with other reported results (8,35,43,44).

Similarly, for each of the constant diameter tests, we show one complete cycle of the axial stretch ratio (Fig. 4h), the axial load (Fig. 4g), the nearly constant external diameter (Fig. 4f), and the luminal pressure required to maintain the diameter constant (Fig. 4e), all plotted vs. time. As expected, increasing axial extensions tend to reduce the external diameter, and the infusion pressure needed to be continuously increased, particularly near the maximum extension, in order to maintain the diameter constant (i.e., within a preselected error band). These data, replotted (Fig. 5b) as axial load vs. extension for three different fixed external diameters, reveal the characteristic nonlinear stiffening behavior exhibited by many soft tissues, as well as the minimal effect of modest changes in external diameter on axial load.

### *Aorta*

Similar tests were performed on descending canine thoracic aortas which were immersed in normal saline at room temperature (29). These tests were accomplished by using different sized end adapters on the mounting rods and by replacing the 200 mm macro lens on the video camera with a 100 mm macro lens. In addition to extension and inflation tests, which revealed vessel behavior consistent with that reported by others (e.g., 39), we also superimposed a cyclic ± 60 degree "twist" on various levels of constant diameters and constant axial extensions. Figure 6 shows data from tests wherein the external diameter was maintained constant at 13 mm (Fig. 6d) while the axial stretch ratio was separately kept constant at 1.6 and 1.7 (Fig. 6e). The pressure (Fig. 6a) and axial load (Fig. 6b) required to maintain the diameter and the axial extension constant, varied little with the superimposed twist (Fig. 6f). The torque (Fig. 6c) vs. twist (per unit unloaded length) data, replotted in Fig. 7a, are nearly linear with small hysteresis. This finding is consistent with the single report in the literature on the torsion of arteries (20). Data from similar tests on the same specimen are in Fig. 7b. They reveal that, as expected, the torque-twist behavior is more sensitive to changes in diameter than changes in axial extension.

Kas'yanov and Rachev (20) showed only the magnitudes of the torque and twist, not the directions. The data in Fig. 7 suggest that both the magnitude and the direction of twist may reveal interesting characteristics of the vessel behavior. For example, a small but non-zero torque was required to maintain the vessel "untwisted" at fixed axial lengths and diameters that were greater than those in the unloaded state (i.e., the vessel would have twisted if it were stretched and inflated with one free end), and cyclic ±60° rotations of one end of the vessel did not yield a symmetric torque-twist behavior. Though provocative, further comment on the torsion behavior of the aorta is beyond the scope of this paper.

## DISCUSSION

### *Protocols*

Many different classes of experiments can, and have been performed on excised blood vessels. These include

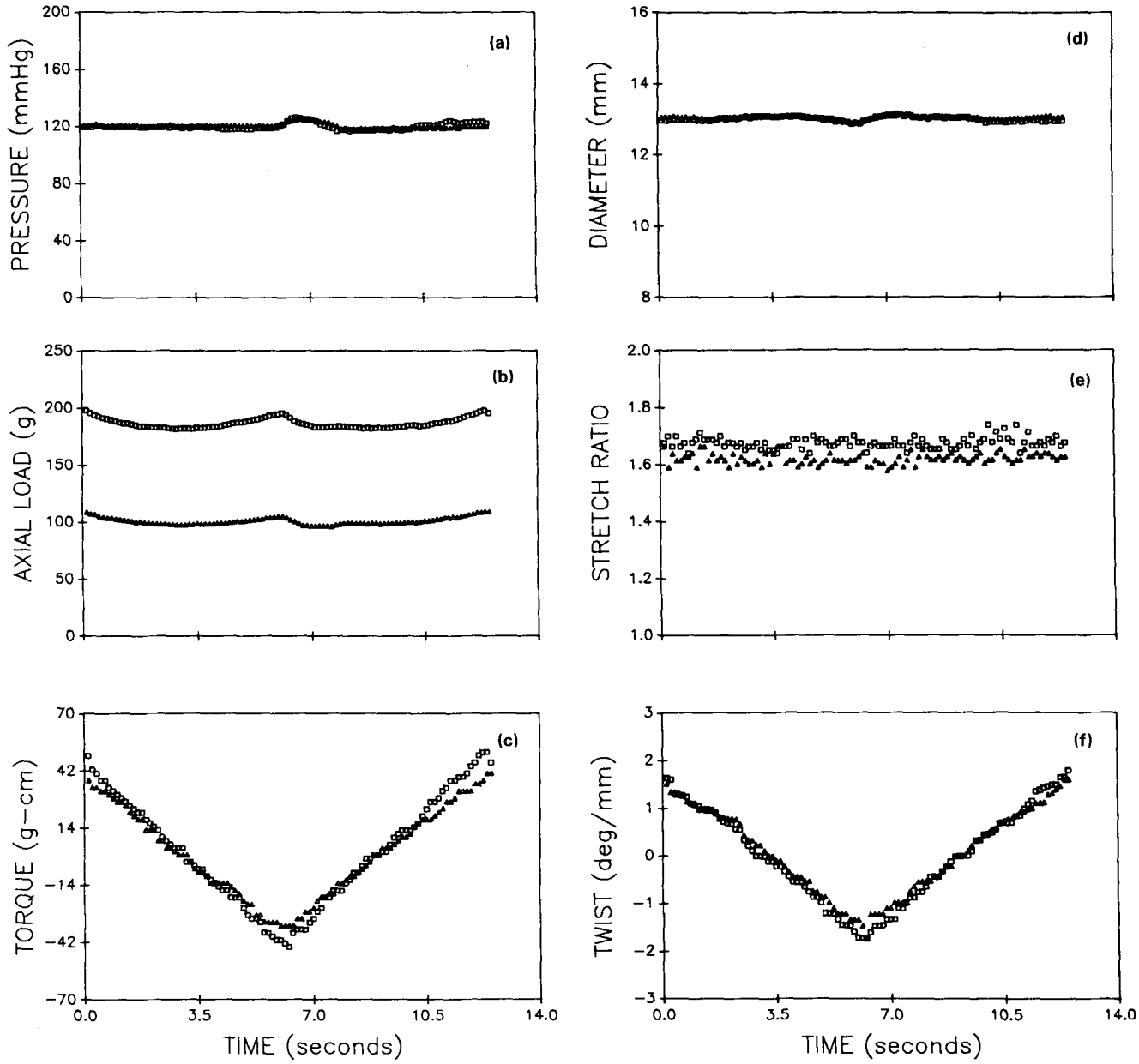


**FIGURE 6. A complete cycle of data from two protocols wherein the external diameter and the axial stretch ratio were both maintained constant during a ±60° cyclic torsion test on a segment of descending thoracic canine aorta.**

the uniaxial extension of rings or strips, the equibiaxial inflation of sheets of vessels, and the cyclic inflation of prestretched cylindrical segments. The latter tests are the most common, since vessels experience these deformations *in vivo*, and one should probably include these "physiologically relevant" inflation tests in any study of vascular mechanics.

Tests which do not correspond directly to *in vivo* deformations must also be considered, however, and theoretical arguments should be used to determine which experiments are the most useful for identifying the general characteristics of the vessel behavior, the specific functional form of the constitutive relation, and the values of the material parameters (18). For example, Humphrey *et al.* (19) performed biaxial tests on thin slabs of excised myocardium wherein one coordinate invariant measure of the finite deformation was maintained constant while another varied, and vice versa. It was shown that even though myocardium does not experience such deformations *in vivo*, these theoretically motivated com-

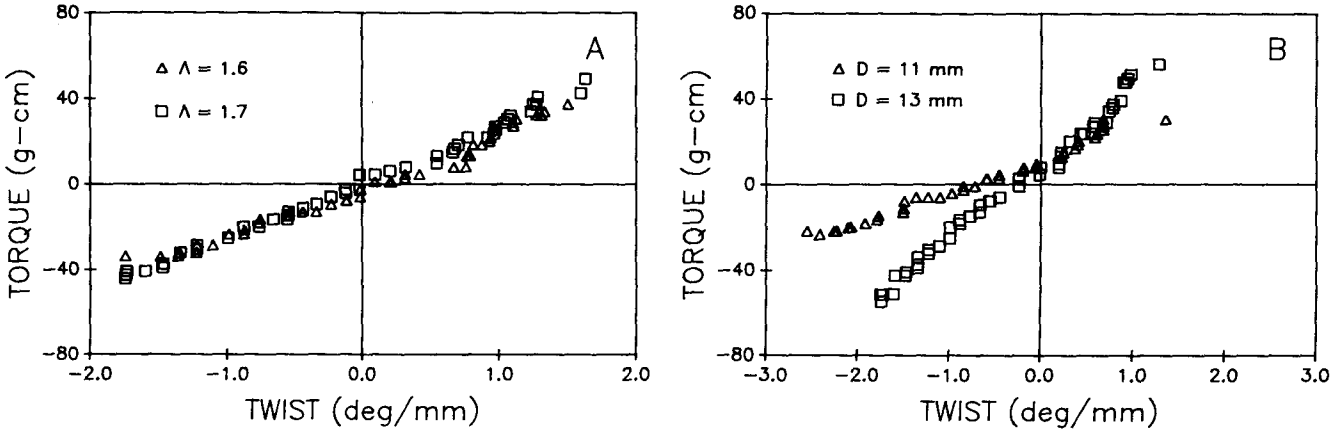


**FIGURE 7. Torque-twist plot of (a) the data in Fig. 6, and (b) data from similar tests.**

puter-controlled tests were very useful in identifying the form of the constitutive relation. Similar theoretically motivated tests have not been performed on blood vessels.

*Previous Devices and Tests*

Perhaps the simplest experiment on a cylindrical vessel consists of suspending the specimen vertically from a stand, hanging weights from a bottom cannula to induce axial extensions, and inflating the vessel with a syringe or a pump (28,34,38). Combined axially "isotonic" and cyclic inflation tests are performed easily in this way. Another common experimental setup consists of mounting a specimen bath vertically on a commercial tensile testing device, and connecting the immersed specimen to the load cell and cross-head (17,31,44). Again the vessel can be inflated with a syringe or a pump. This setup allows simultaneous cyclic extension and inflation tests. Similar tests were reported by van Loon *et al.* (39) who employed a custom extension apparatus rather than a commercial tensile testing device; axial extensions were induced by a cam system driven by a harmonic generator.

Custom experimental devices exist wherein vessels are mounted horizontally in a specimen bath with one cannula attached to a fluid pump and pressure transducer and another cannula connected to an axial load cell and a manually movable frame or slide (5,8,11,35,43). The methods of deformation measurement vary in these reports, and include LVDT measurement of overall specimen length, contacting diameter transducers, and VDAs for both diameter and gage length measurement. Clearly, these devices are well suited for performing cyclic inflation tests at fixed axial extensions or loads, that is, "physiologic tests."

Few of these experimental setups utilize on-line data collection or noncontacting measurements of the deformations in a central gage length, and none are completely under computer control. Rather, control is through open-loop function generator control of the axial extensions in the tensile testers, and the closed-loop pressure control of the vessel inflation afforded by Harvard Apparatus pumps (5,43). Computer control provides more flexibility in performing different protocols, it increases experimental reproducibility, it minimizes human error, and it simplifies execution. This is not to say that non-computer controlled experiments are undesirable—much has been learned from these tests. Nonetheless, computer-controlled tests promise to provide new insights into vascular behavior, and thus constitutive relations, by allowing newer, more general experimental protocols to be performed and quantified.

The only previous computer-controlled device capable of simultaneously extending and inflating a blood vessel was reported by Vito (41). Briefly, Vito's device consists of a DC servo motor, connected to coupled left- and right-hand ball screws, which drives two metallic lead carriages in opposite directions. An axial load cell and specimen mounting rods ride atop the carriages, and the specimen is inflated using a stepper motor driven pump. Gage length deformations are measured optically with a CCD camera and a dedicated video system. Data are collected on-line and are used for feedback control of the experiments. For example, data from "constant diameter" tests on seven canine aortas were presented by Vito and Hickey (42).

Our present design is similar to Vito's device in many ways. In fact, we benefited greatly from Vito's report. Nonetheless, our device differs from Vito's device in that (a) our mechanical axes lie in a horizontal plane rather than a vertical one (this allows easier access to all machine parts and decreases the potential for corrosion of the parts by saline); (b) our singly constructed, twin shaft/carriage

system is stiffer in the stretching plane, it minimizes alignment problems, and it appears to transmit less noise from the motors and ball screws to the specimen and transducers; (c) our device is capable of twisting cylindrical vessels; and (d) we employed newer, faster video and stepper motor technology. It appears that our device is the only one presently capable of performing simultaneous extension, inflation, and torsion tests on blood vessels completely under computer control.

### *Experimental Data*

It was not our intent to present data that reveal new information on vascular behavior. Rather, data were presented only to illustrate some of the tests which can be performed easily with our new device and the associated information which can be collected on-line. Thus, we simply note that the vascular behavior illustrated in Figs. 4 and 5 is consistent with that which has been reported by many investigators, whereas the data in Figs. 6 and 7 suggest that future torsion tests may yield new, important information on vascular behavior.

### *Conclusion*

The identification of classes of experiments that are potentially useful for studying vascular behavior should be based on theoretical constructs or physiological relevance, not convenience, prior bias, or restrictions imposed by an apparatus. We designed and assembled a new computer-controlled system for subjecting cylindrical segments of artificial or excised natural blood vessels to simultaneous inflation, extension, and torsion tests. This device is capable of performing a broader class of tests on vessels than heretofore possible, and thus should allow new theoretically motivated tests to be performed for the first time. There is a need, therefore, to continue to identify which tests should be performed on which vessels. Finally, we recognize that many tests will not be able to be performed even with this new system. Thus, when needed, new complementary devices should be designed and built. Only by continuing to improve our theoretical foundations and our experimental facilities will we be able to discover and quantify new aspects of vascular behavior, which in turn will lead to a better understanding of clinically important problems.

## REFERENCES


1. Bergel, D.H. Mechanics of the arterial wall in health and disease. In: Bauer, R.D.; Busse, R.; eds. The arterial system. Berlin, Germany: Springer-Verlag. 1978.
2. Canfield, T.R.; Dobrin, P.B. Static elastic properties of blood vessels. In Skalak, R.; Chien, S., eds. Handbook of bioengineering. New York: McGraw-Hill. 1987.
3. Castaneda-Zuniga, W.R.; Sibley, R.; Amplatz, K. The pathologic basis of angioplasty. Angiol. 35:195-205, 1984.
4. Consigny, P.M.; Tulenko, T.N.; Nicosia, R.F. Immediate and long-term effects of angioplasty-balloon dilation on normal rabbit iliac artery. Arterioscl. 6:265-276; 1986.
5. Cox, R.H. Three-dimensional mechanics of arterial segments *in vitro*: Methods. J. Appl. Physiol. 36:381-384; 1974.
6. Cox, R.H. Regional variation of series elasticity in canine arterial smooth muscle. Am. J. Physiol. 234:H542-H551; 1978.
7. Cox, R.H. Comparison of arterial wall mechanics using ring and cylindrical segments. Am. J. Physiol. 244:H298-H303; 1983.
8. Dobrin, P.B. Biaxial anisotropy of dog carotid artery: Estimation of circumferential elastic modulus. J. Biomech. 19:351-358; 1986.
9. Dobrin, P.B. Mechanisms and prevention of arterial injuries caused by balloon embolectomy. Surg. 106:457-466; 1989.
10. Downs, J.; Halperin, H.R.; Humphrey, J.D.; Yin, F.C.P. An improved video-based computer tracking system for soft biomaterials testing. IEEE Trans. Biomed. Engr. 37:903-907; 1990.
11. Fronek, K.; Schmid-Schoenbein, G.; Fung, Y.C. A noncontact method for three-dimensional analysis of vascular elasticity *in vivo* and *in vitro*. J. Appl. Physiol. 40:634-637; 1976.
12. Fronek, K.; Fung, Y.C. Mechanical properties of arteries as a function of topography and age. Biorheol. 17:227-234; 1980.
13. Fung, Y.C.; Fronek, K.; Patitucci, P. Pseudoelasticity of arteries and the choice of its mathematical expression. Am. J. Physiol. 237:H620-H631; 1979.
14. Fung, Y.C. Biomechanics: Mechanical properties of living tissues. Berlin, Germany: Springer-Verlag; 1981.
15. Goldberg, E.M.; Goldberg, M.C.; Chowdhury, L.N.; Gould, S.A. The effects of embolectomy-thrombectomy catheters on vascular architecture. J. Cardiovasc. Surg. 24:74-80;1983.
16. Hayashi, K.; Nakamura, T. Material test system for the evaluation of mechanical properties of biomaterials. J. Biomed. Matl. Res. 19:133-144; 1985.
17. How, T.V.; Clarke, R.M. The elastic properties of a polyurethane arterial prosthesis. J. Biomech. 17:597-608; 1984.
18. Humphrey, J.D.; Strumpf, R.K.; Yin, F.C.P. A theoretically based experimental approach for identifying vascular constitutive relations. Biorheol. 26:687-702; 1989.
19. Humphrey, J.D.; Strumpf, R.K.; Yin, F.C.P. Determination of a constitutive relation for passive myocardium: I. The functional form. ASME J. Biomech. Engr. 112:333-339; 1990.
20. Kas'yanov, V.A.; Rachev, A.I. Deformation of blood vessels upon stretching, internal pressure and torsion. Mech. Comp. Matls. 16:76-80; 1980.
21. Lee, J.S.; Fraser, W.G.; Fung, Y.C. Comparison of elasticity of an artery *in vivo* and in excision. J. Appl. Physiol. 25:799-801; 1968.
22. Lyon, R.T.; Zarins, C.K.; Lu, C.T.; Yang, C.F.; Glagov, S. Vessel, plaque and lumen morphology after transluminal balloon angioplasty. Arterioscl. 7:306-314; 1987.
23. Mohan, D.; Melvin, J.W. Failure properties of passive human aortic tissue. I—Uniaxial tension tests. J. Biomech. 15:887-902; 1982.
24. Mohan, D., Melvin, J.W. Failure properties of passive human aortic tissue. II—Biaxial tension tests. J. Biomech. 16:31-44; 1983.

25. Nahon, D.; Lee, J.M. A two-dimensional incremental study of the static mechanical properties of vascular grafts. Clin. Matls. 1:177–197; 1986.
26. Ostergaard, J.R.; Oxlund, H. Collagen type III deficiency in patients with rupture of intracranial saccular aneurysms. J. Neurosurg. 67:690–696; 1987.
27. Patel, D.J.; Fry, D.L. Longitudinal tethering of arteries in dogs. Circ. Res. 19: 1011–1021; 1966.
28. Patel, D.J.; Janicki, J.S. Static elastic properties of the left coronary circumflex artery and the common carotid artery. Circ. Res. 27:149–158; 1970.
29. Patel, D.J.; Vaishnav, R.N. Basic hemodynamics and its role in disease processes. Baltimore, MD: University Park Press; 1980.
30. Quigley, M.R.; Heiferman, K.; Kwaan, H.C.; Vidovich, D.; Nora, P.; Cerullo, L.J. Bursting pressure of experimental aneurysms. J. Neurosurg. 67:288–290; 1987.
31. Sato, M.; Niimi, H.; Okumura, A.; Handa, H.; Hayashi, K.; Moritake, K. Axial mechanical properties of arterial walls and their anisotropy. Med. Biol. Eng. Comput. 17:170–176; 1979.
32. Sharma, M.G.; Hollis, T.M. Rheological properties of arteries under normal and experimental hypertension conditions. J. Biomech. 9:293–300; 1976.
33. Stewart, S.F.C.; Lyman, D.J. Essential characteristics of vascular grafts. In: Sawyer, P.N., ed. Modern vascular grafts. New York: McGraw-Hill; 1987.
34. Stewart, S.F.; Lyman, D.J. Predicting the compliance of small diameter vascular grafts from uniaxial tensile tests. J. Biomech. 23:629–637; 1990.
35. Takamizawa, K.; Hayashi, K. Strain energy density function and uniform strain hypothesis for arterial mechanics. J. Biomech. 20:7–17; 1987.
36. Thubrikar, M.J.; Baker, J.W.; Nolan, S.P. Inhibition of atherosclerosis associated with reduction of arterial intraluminal stress in rabbits. Arterioscl. 8:410–420; 1988.
37. Vaishnav, R.N. Mathematical characterization of the nonlinear rheological behavior of the vascular tissue. Biorheol. 17:219–226; 1980.
38. Vaishnav, R.N.; Vossoughi, J.; Patel, D.J.; Cothran, L.N.; Coleman, B.R.; Ison-Franklin, E.L. Effect of hypertension on elasticity and geometry of aortic tissue from dogs. ASME J. Biomech. Eng 112:70–74; 1990.
39. van Loon, P.; Klip, W.; Bradley, E.L. Length-force and volume-pressure relationships in arteries. Biorheol. 14:181–201; 1977.
40. Vinall, P.E.; Simeone, F.A. Whole mounted pressurized *in vitro* model study of cerebral arterial mechanics. Blood Vessels 24:51–62; 1987.
41. Vito, R.P. The mechanical properties of soft tissues: I. A mechanical system for biaxial testing. J. Biomech. 13:947–950; 1980.
42. Vito, R.P.; Hickey, J. The mechanical properties of soft tissues: II. The elastic response of arterial segments. J. Biomech. 13:951–957; 1980.
43. von Maltzahn, W.W.; Warriyar, R.G.; Keitzer, W.F. Experimental measurements of elastic properties of media and adventitia of bovine carotid arteries. J. Biomech. 17:839–847; 1984.
44. Weizsacker, H.W.; Lambert, H.; Pascale, K. Analysis of the passive mechanical properties of rat carotid arteries. J. Biomech. 16:703–715; 1983.
45. Yin, F.C.P.; Tompkins, W.R.; Peterson, K.L.; Intaglietta, M. A video dimension analyzer. IEEE Trans. Biomed. Eng. 19:376–381; 1972.
46. Yin, F.C.P.; Spurgeon, H.A.; Kallman, C.H. Age associated alterations in viscoelastic properties of canine aortic strips. Circ. Res. 53:464–472; 1983.